Interfacial Mixing by Horizontal Vortices and Shear Turbulence

J. B. Flór, E.H. Hopfinger, and E. Guyez

Laboratoire des Ecoulement Geophysiques et Industriels LEGI-CNRS, B.P.53X, 38041 Grenoble Cedex 09, France, Jan-Bert.Flor@hmg.inpg.fr, Emil.Hopfinger@legi.grenoble-inpg.fr, E.M.C.Guyez@warwick.ac.uk

Summary. In this paper the entrainment rates of shear flows and turbulent Taylor vortices are considered in the light of the mixed-layer deepening in oceans, seas and lakes. The entrainment by Taylor vortices can be considered to represent a model for entrainment by continuously driven horizontal vortices such as Langmuir circulation. When the forcing is related to the surface wind stress, the interfacial entrainment by Langmuir vortices can be estimated from the experimental results on turbulent Taylor vortices, and compared with the entrainment rates in pure shear-flows. The results indicate that mixing by Langmuir vortices is important for all Richardson numbers, Ri_* (based on wind-induced surface stress velocity), and that for $Ri_* > 80$ Langmuir vortices dominate the mixed-layer deepening.

1 Introduction

The mixing of the surface layer of the ocean is of relevance for ocean-atmosphere exchange of heat, mass and momentum, and has been a major motivation for many studies on mixing of stratified fluids. The vertical fluid exchange and mixing of the surface layer in water basins and lakes is also relevant to the water quality in view of the transport of biological and chemical compounds. The relevance of Langmuir circulation to the mixed surface layer deepening is not fully understood (see Thorpe [11]). In this paper, experimental results on entrainment in turbulent shear flows and Taylor vortices are compared. Details of this study can be found in Flór et al. [2].

Langmuir cells consist of an array of alternating horizontal vortices at the ocean surface that are aligned with the wind direction. These cells establish due to the combined action of wind-induced shear and of Stokes drift (see reviews of Leibovich [6]; Thorpe [11]) and may have a depth between 2 and 300 m with an aspect-ratio close to 1. Typical velocities range from 10 to 20 cm/s for wind speeds of 3–5 m/s or larger (see e.g. Smith [9]; Weller and Price [12]; Thorpe [11]).

A.D. Fitt et al. (eds.), *Progress in Industrial Mathematics at ECMI 2008*, Mathematics in Industry 15, DOI 10.1007/978-3-642-12110-4_41,

In order to estimate the relevance of the mixing process of shear turbulence relative to Langmuir circulation, Li et al. [7] suggested that the mixing stops for a critical Froude number given by

$$Fr = \frac{w_{dn}}{(h\Delta b)^{1/2}} = C \tag{1}$$

where w_{dn} is the maximum downwelling velocity, $\Delta b = g\Delta\rho/\rho$ the buoyancy jump at the base of the mixed layer and h the mixed layer depth. Li et al. [7] suggest for the value C, 0.9 for a two-layer and 0.6 for a linearly stratified fluid. For the shear instability they employed the Price et al. model which predicts static stability of the mixed layer when

$$Ri_b = \frac{\Delta bh}{(\Delta U)^2} \geq 0.65. \tag{2}$$

with mean velocity difference across the density interface at the base of the mixed layer ΔU. Then the transition from Langmuir mixing to shear mixing was predicted to be

$$w_{dn}/C \geq \sqrt{0.65}\Delta U. \tag{3}$$

As far as the measurement resolution allows, in situ measurements confirmed that Langmuir vortices may dominate the dynamics when this criterion is fulfilled.

This criterion is based on laminar vortices, for which the mixing is arrested above the critical Froude number. For turbulent vortices, the mixing may continue on a smaller scale even for large Froude numbers because of the presence of smaller scales. In order to know how relevant this mixing is compared to shear turbulence it is essential to know the entrainment rates of both processes. In this context we consider the entrainment rates measured in different laboratory studies. A sketch of these different laboratory flows is presented in Fig. 1.

2 Experiments on Shear- and Vortex-Induced Mixing

A Taylor-Couette device consists of two concentric cylinders with the inner cylinder rotating and centrifugal instability leads to the formation of so-called Taylor vortices of the size of the gap width (see Fig. 1). Supposing that the side walls act as symmetry planes in the horizontal direction, the Taylor vortices above the interface have essential aspects in common with Langmuir vortices.

In these measurements the entrainment rate was measured from the vertical density flux (see Guyez et al. [3] for details)

$$F(z,t) = \int_z^h \frac{\partial\rho(z,t)}{\partial t} dz.$$

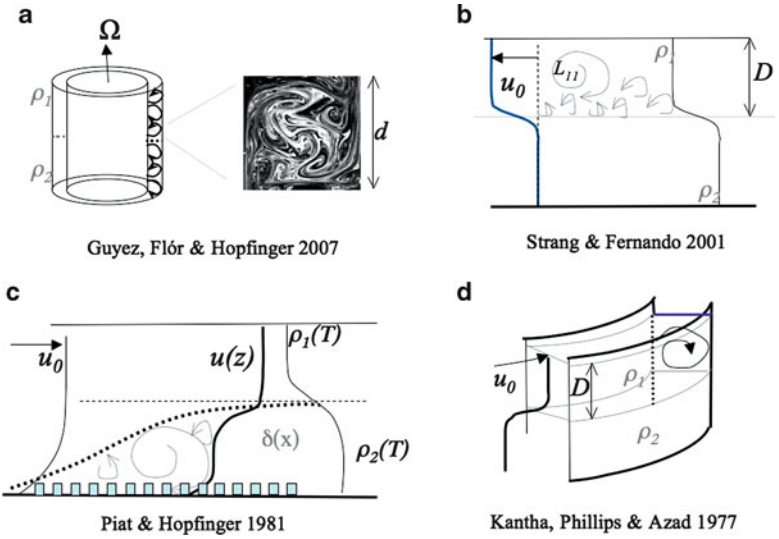

Fig. 1. Schematic diagram of the different experimental flows considered, with (**a**) the Taylor Couette flow and Taylor vortices, (**b**) the shear flow in the Odell-Kovasznay device (see Strang and Fernando [10]) (**c**) a wind induced shear flow and (**d**) the shear flow driven by an annular disk at the fluid surface

At the boundaries $z = 0$ and $z = h$ the flux is zero so that when the interface is thin and is bounded above and below by mixed layers, the flux decreases linearly above and below the interface. The flux can be expressed in terms of an entrainment velocity u_e across the interface in the form $F(z_{int}, t) = \Delta\rho(t)u_e(t)$ from which the entrainment rate u_e/u_m with maximum velocity u_m was calculated. Figure 2 (lower curve) is the entrainment rate as a function of the Richardson number here defined as $Ri_* = \Delta bd/u_m^2$ and d the size of the vortex.

To relate the entrainment rates of Langmuir vortices to that of Taylor vortices, we use the estimations of Li et al. [7] for the surface friction-velocity, u_*, induced by the wind at the surface, U_w, and the maximum down welling velocity w_{dn}. These relations are based on in situ measurements and are $u_* = 1.3 \cdot 10^{-3} U_w$, and $w_{dn} = 8.3 \cdot 10^{-3} U_w$ yielding for the maximum down-welling velocity $w_{dn} = 6.4u^*$. Relating the maximum down-welling velocity to the maximum vertical velocity in the Taylor vortices, $u_m \approx w_{dn} = 6.4u^*$ one obtains the upper curve in Fig. 2, showing the entrainment rate and Richardson number of the Taylor vortices relative to the wind friction velocity u^*.

In the Taylor–Couette flow the interface stays at approximately the same height because of the forcing symmetry below and above the interface. Since the mixing is invariant to forcing at both sides or a single side of the interface (see Turner 1968) we may consider a single vortex above the interface. If the

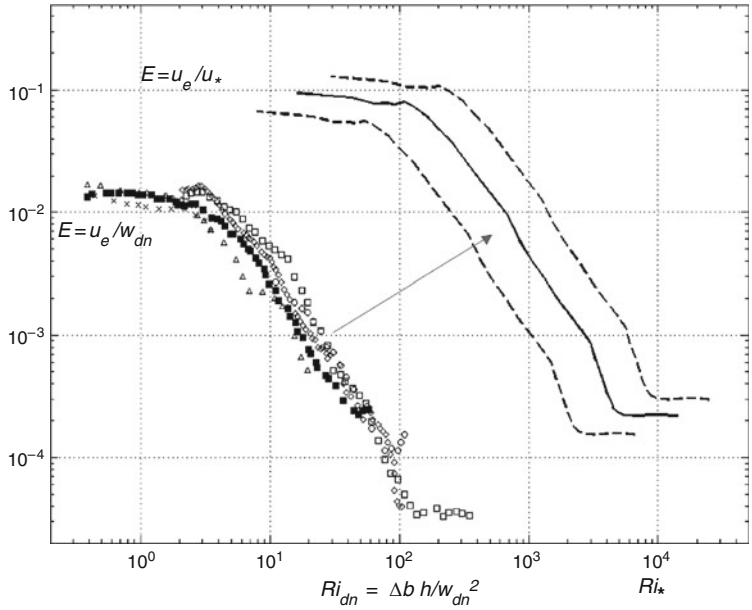

Fig. 2. Entrainment coefficient E versus Richardson number Ri_{dn} and Ri_*. Dashed lines represent the lower and upper limits of the entrainment (see Flór et al. [2])

vortices could be generated only above the interface, the mixed layer would deepen by the turbulent vortex near the interface with a rate $F/\Delta\rho$ over a depth d. This entrainment rate is therefore comparable to the entrainment rate based on the layer deepening as measured in the shear flows discussed below (for a detailed discussion on the different entrainment rates see Hunt et al. [4]).

In shear flows the fluid at the interface mixes due to shear instabilities (Kelvin Helmholtz instability and for larger Richardson numbers Holmboe instability, see Strang and Fernando [10]), and large scale motions continuously homogenize the upper layer. A sketch of a shear flow in which the upper layer is moving over a denser lower layer is shown in Fig. 1b. The entrainment rate is measured from the increase in upper-layer depth and is scaled with the *rms* velocity. This velocity is approximately equal to the surface friction velocity u_*. As typical length scale the integral length scale of the mixing eddies L_{11} is taken (see Strang and Fernando [10]), so that one obtains a Richardson number $Ri_* = \Delta b L_{11}/u_*^2$.

The configuration of a boundary layer topped by a density interface considered by Piat and Hopfinger [8] is analogue to a wind induced shear flow in a mixed surface layer limited by a pycnocline. The experiments were conducted

in a wind tunnel, with the two-layer stratification set by temperature difference. The turbulent boundary layer was generated by roughness elements at the bottom boundary so that with distance from the inlet of the tunnel, the boundary layer increased in thickness until it mixed the interface and thus increased the lower layer thickness. The entrainment velocity varied with distance and was defined as $u_e = (dD(x)/dx)U_0$, with U_0 the background velocity and $D(x)$ the mixed layer depth. The friction velocity here induced by the bottom roughness was taken as typical velocity yielding a Richardson number $Ri_* = \Delta bh/u_*^2$ and entrainment rate $E = u_e/u_*$.

Another type of shear flow is one that is driven by the rotation of an annular disk at the surface of a two-layer salt-stratified fluid (see Fig. 1d) (see Kantha et al. [5]). Because of the secondary circulation generated by the fluid accelerated in the viscous boundary layer of the annular disk, later studies rejected these results since essentially different from pure shear flows. In the present context, however, these results can be considered as intermediate between a pure shear flow, and the pure vortex driven entrainment in Taylor-Couette flow. The entrainment rate is again based on layer deepening dh/dt, whereas the Richardson number is defined as $Ri_* = \Delta bh/u_*^2$ with u_* the surface friction velocity.

3 Comparison of Results and Discussion

Figure 3 shows the different results for the entrainment rate dimensioned with the surface friction velocity as a function of Ri_*. For $Ri_* < 80$ shear induced entrainment dominates over the Langmuir vortex induced entrainment by approximately a factor 2 or less. At the crossover $Ri = 80$ shear instabilities are arrested by the stratification and the entrainment rate drops off to very low values whereas turbulent vortices continue the mixing on smaller scales, thus explaining the higher entrainment rates for Langmuir circulation. The entrainment rates obtained by Kantha et al. [5] follow the shear turbulence for $Ri < 80$ and the Langmuir turbulence for $Ri > 80$ and are coherent with the present findings. For higher Ri_* numbers it drops of slightly faster than the purely vortex driven flow because the secondary circulation in Kantha et al.'s experiments must be relatively weak compared to the rather turbulent Taylor vortices. Deardorff and Yoon [1], who considered the flow in an annular tank driven by an annular disk that did not entirely cover the fluid surface as a mean to reduce the secondary circulation. For $Ri > 80$, their results (not plotted in the figure) fall in between those of Strang and Fernando [10] and Kantha et al. [5], again in coherence with the relatively higher vortex-entrainment rates for large Ri-numbers.

Observations confirm this tendency of an initial layer deepening due to shear instability and subsequent deepening due to Langmuir cells. For a pycnocline with typically $\Delta b = 3 \cdot 10^{-3}\,\mathrm{m\,s^{-2}}$, 1 m depth and $5m/$ wind speed (i.e. $u_* = 0.65\ 10^{-2}\,\mathrm{m/s}$) this implies a Richardson number of $Ri_* \approx 72$ with

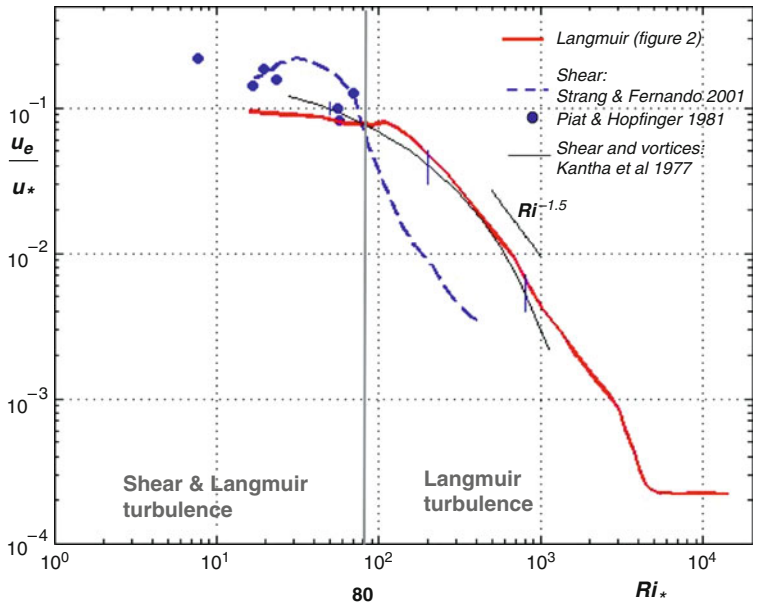

Fig. 3. Entrainment rates dimensioned with the wind-induced surface shear-stress u_* as a function of Ri_*. The error bars in the data are estimated from the data sets

deepening mainly due to Langmuir vortex cells for larger layer depths. Langmuir cells typically obtain a depth of approximately 20 m or larger, suggesting a dominant effect of Langmuir circulation on mixed layer deepening.

References

1. Deardorff, J.W., Yoon, S.-C.: J. Fluid Mech. **142**, 97–120 (1984)
2. Flór, J.B., Hopfinger, E.J., Guyez, E.J.: Deep Sea Res.: submitted (2008)
3. Guyez, E.J., Flór, J.B., Hopfinger, E.J.: J. of Fluid Mech. **46**, 11–21 (2007)
4. Hunt, J.C.R., Rottman, J.W., Britter, R.E.: IUTAM Symposium 1983 Atmospheric Dispersion of Heavy Gases and Small Particles, pp. 361–395. (1984)
5. Kantha, L.H., Phillips, O.M., Azad, R.S.: J. Fluid Mech. **79**, 753–768 (1977)
6. Leibovich, S.: Ann. Rev. Fluid Mech. **15**, 391–427 (1983)
7. Li, M., Zahariev, K., Garrett, C.: Science **270**, 1955–1957 (1995)
8. Piat, J.-F., Hopfinger, E.J.: J. Fluid Mech. **113**, 411–432 (1981)
9. Smith, J.A.: J. Geophys. Res. **103**, 12.649–12.668 (1998)
10. Strang, E.J., Fernando, H.J.S.: J. Fluid Mech. **428**, 349–386 (2001)
11. Thorpe, S.A.: Ann. Rev.Fluid Mech. **36**, 55–79 (2004)
12. Weller, R.A., Price, J.F.: Deep Sea Res. **35**, 711–47 (1988)
13. Turner, J.S., J. Fluid Mech. **33**, 639–656 (1968)